

# Quarkonium production and suppression in Pb+Pb and p+A collisions at SPS energies

L. Ramello<sup>a</sup> (for the NA50\* Collaboration)

<sup>a</sup>Università del Piemonte Orientale, Alessandria and INFN-Torino, Italy

We present the results on charmonium production as measured by experiment NA50 at the CERN-SPS in p+A and Pb+Pb collisions. The  $J/\psi$  / Drell-Yan and  $\psi'$  / Drell-Yan cross-section ratios as a function of centrality are obtained from Pb+Pb data samples collected at 158 GeV per nucleon in the 1998 run and, under improved experimental conditions, in 2000. The recent very high precision NA50 proton-nucleus results allow to determine the  $J/\psi$  nuclear absorption only from proton induced reactions, and to calculate the expected  $J/\psi$  yield in Pb+Pb collisions at 158 GeV. The  $J/\psi$  expected production obtained in this way is compared to the NA50 results in Pb+Pb collisions, as well as to the NA38 results for S+U reactions.

## 1. INTRODUCTION

Charmonium production in heavy ion collisions is a prominent tool to test whether deconfinement has occurred; in fact  $J/\psi$  suppression was predicted on the basis of quark-gluon plasma (QGP) colour screening [1] already before the start of the CERN SPS experimental programme. An up-to-date assessment of the theoretical status of  $J/\psi$  suppression is given in [2].

Early measurements by the NA38 experiment with p+A, O+U and S+U collisions performed in the years 1986-1992 provided evidence for  $J/\psi$  suppression, which however was finally understood [3] as due to absorption in ordinary nuclear matter. The NA50 experiment found the first evidence for the  $J/\psi$  anomalous suppression [4,5] in central Pb+Pb collisions at 158 GeV/nucleon with the data collected in 1995-1996. In this paper we present the measurement of the  $J/\psi$  and  $\psi'$  yields as a function of collision centrality, from data collected in years 1998 and 2000; the Drell-Yan process cross-section, experimentally shown to be proportional to the number of nucleon-nucleon collisions, is used for normalization purposes. The  $p_T$  dependence of the  $J/\psi$  suppression has also been studied in order to gain further insight into the anomalous suppression mechanism. Preliminary analyses have been presented earlier [6–8] and the Pb+Pb results on  $J/\psi$  have been recently published [9]; a full account of the  $J/\psi$  suppression measurements at CERN SPS is given in [10].

Thanks to the high statistics of muon pairs collected in p+A interactions, a study of  $\Upsilon$  and high mass Drell-Yan has been performed [11], which can provide a baseline for  $\Upsilon$

---

\*For the full list of NA50 authors and acknowledgments, see appendix 'Collaborations' of this volume.

suppression studies to be carried out in ion-ion collisions at higher center of mass energies.

## 2. DATA TAKING CONDITIONS AND ANALYSIS

The NA50 apparatus has been described elsewhere (see e.g. [9,12]). It consists of a dimuon spectrometer, with the target region equipped with a beam hodoscope and three centrality detectors: the silicon Multiplicity Detector (MD), the Electromagnetic Calorimeter (EMC) and the Zero Degree Calorimeter (ZDC). The corresponding centrality variables are charged multiplicity  $N_{\text{ch}}$ , transverse energy  $E_T$  and forward energy  $E_{\text{ZDC}}$ . Significant improvements to the experimental apparatus were introduced in years 1998 and 2000 in order to avoid reinteractions and Pb-air parasitic interactions (see [6,9]). To address the first problem, already in the 1998 Pb+Pb run a single target configuration was adopted. For the 2000 Pb+Pb run the target region was put under vacuum, a new method based on the EMC signal was developed to detect double interactions and a new target identification method was adopted, based on the two planes of the MD.

The data selection, aimed at rejecting parasitic interactions, double interactions and muons not originating from the target, is fully described in [9]. Data were analyzed using the standard NA50 method which includes a fit to the  $\mu^\pm\mu^\pm$  mass spectra to determine the combinatorial background, a multi-step fit to the  $\mu^+\mu^-$  mass spectra to extract  $J/\psi$ ,  $\psi'$ , Drell-Yan and Open Charm yields and an acceptance correction, and which leads to the cross section ratios  $B_{\mu\mu}\sigma(J/\psi)/\sigma(DY)$  and  $B'_{\mu\mu}\sigma(\psi')/\sigma(DY)$ .

All available NA50 p+A data samples [13–15] have been used to establish the normal nuclear absorption pattern, as described in the next section. Both Pb+Pb and p+A data were analyzed in a coherent way using the most updated resonance line shapes and the GRV 94 LO [16] parton distribution functions to describe the Drell-Yan component.

## 3. A NEW REFERENCE FOR $J/\psi$ NORMAL NUCLEAR ABSORPTION

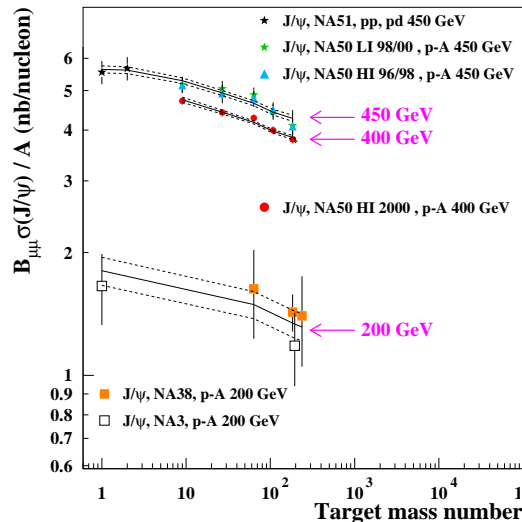


Figure 1. The  $J/\psi$  absolute cross-section (divided by  $A$ ) vs.  $A$  in p+A collisions.

To establish the pattern of  $J/\psi$  normal nuclear absorption vs. centrality for the Pb+Pb

system at 158 GeV/nucleon, since we lack a direct measurement in p+A at that energy, we have developed a procedure which makes use of p+A data obtained at higher energies. This procedure is based on NA50  $J/\psi$  / Drell-Yan p+A results at 450 GeV [13,14] and 400 GeV [15] and on absolute  $J/\psi$  cross-section results from the above data samples as well as (at 200 GeV) from experiments NA3 [17] and NA38 [3].

Figure 1 presents the absolute cross-section measurements, together with the result of a simultaneous Glauber fit with a common value of the  $J/\psi$  absorption cross section  $\sigma_{\text{abs}}^{J/\psi}$  and separate normalizations for each energy and kinematical domain. The result of the fit is  $\sigma_{\text{abs}}^{J/\psi} = 4.48 \pm 0.42$  mb,  $N_{200}/N_{450} = 0.320 \pm 0.025$  and  $N_{200}/N_{400} = 0.357 \pm 0.027$ . If we perform, instead, a Glauber fit to the  $J/\psi$  / Drell-Yan ratios (available only at 450 and 400 GeV) we obtain  $\sigma_{\text{abs}}^{J/\psi} = 4.18 \pm 0.35$  mb, in fair agreement with the previous determination. We use the latter value to fix the shape of the absorption curve vs. centrality.

Concerning the normalization of the absorption curve we proceed as follows: (i) we start from the  $J/\psi$  / DY normalization at 450 GeV (1.4% error); (ii) we rescale to 200 GeV using the measured absolute  $J/\psi$  cross-sections quoted above (7.8% error including systematics) and a leading order calculation for the Drell-Yan cross-section (2.5% error); (iii) we rescale to 158 GeV using a fit to measured  $J/\psi$  production cross-sections in pp and  $\bar{p}p$  collisions vs.  $\sqrt{s}$  (1.5% error) and a LO calculation for the Drell-Yan cross-section.

We then perform a Glauber calculation which includes experimental smearing to express the absorption curve in terms of the Pb+Pb centrality variables; the spatial distributions of protons and nucleons in different nuclei are parametrized according to experimental results, including recent evidence for the so-called neutron halo [18] in heavy nuclei. Our main assumption, supported by available data, is that  $\sigma_{\text{abs}}^{J/\psi}$  is the same in p+A collisions ranging from 158 to 450 GeV. The absorption curve is, on the other hand, completely independent of S+U data. It is shown together with Pb+Pb results in the next section.

## 4. RESULTS

### 4.1. Centrality dependence of the $J/\psi$ / DY cross-section ratio

We start by presenting the  $J/\psi$  / DY cross-section ratio in Pb+Pb as a function of  $E_T$ . Figure 2 shows the 2000 data (from [9]) with the absorption curve at 158 GeV determined according to the procedure used in [6–8], which relied also on S+U data for the normalization. The error on the absorption curve is only about 4% at the expense of assuming that the  $J/\psi$  in S+U interactions undergoes the same nuclear absorption as in p+A. Figure 3 (also from [9]) shows the same data compared to the absorption curve determined from p+A data only: the error is larger, about 8-9%, but we are free from the above assumption. We note that the absorption curve itself is almost the same with both procedures. Inserts show the ratio “measured/expected”.

We then compare in Fig. 4 the  $J/\psi$  suppression pattern vs.  $E_T$  from the 1998 and 2000 data samples; we observe that they are compatible, allowing us to present in Fig. 5 the averaged result, which represents the highest statistical precision obtained in NA50 with the standard  $J/\psi$  / DY method. From this result we confirm the departure from normal nuclear absorption at mid-centrality and the steady decrease of the  $J/\psi$  / DY ratio up to the highest centrality.

Two independent analyses as a function of the centrality variables  $N_{\text{ch}}$  (Fig. 6) and

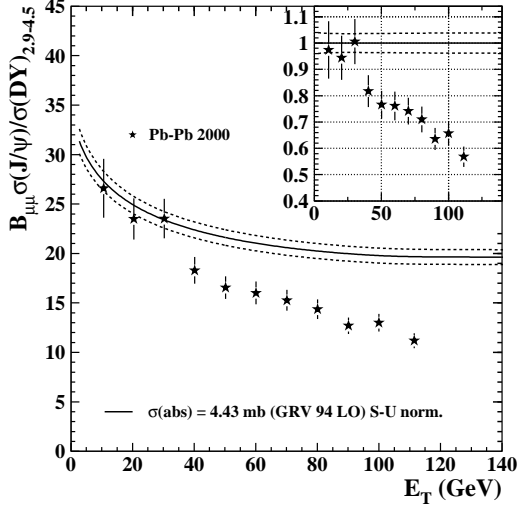


Figure 2. The  $J/\psi/DY$  ratio vs.  $E_T$  from year 2000 data. Absorption curve determined from p+A and S+U data.

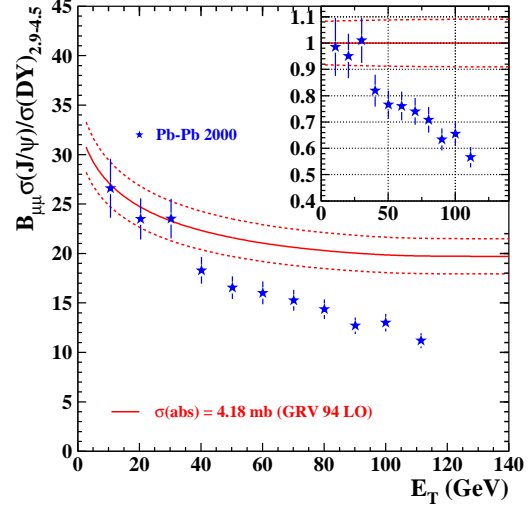


Figure 3. The  $J/\psi/DY$  ratio vs.  $E_T$  from year 2000 data. Absorption curve determined from p+A data only.

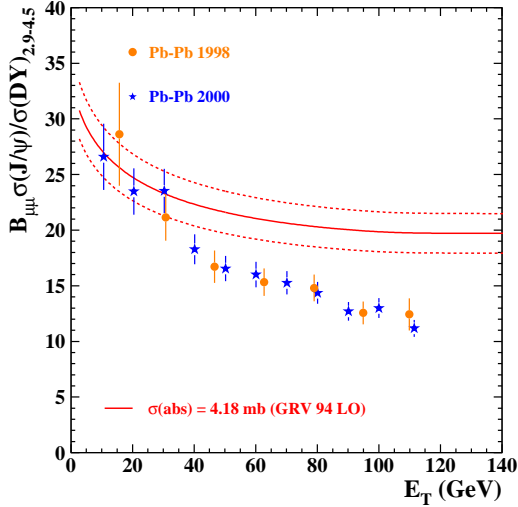


Figure 4. The  $J/\psi/DY$  ratio vs.  $E_T$ : NA50 data from years 1998 and 2000.

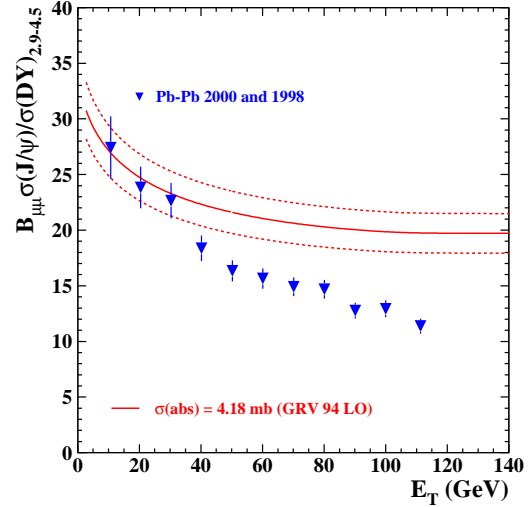


Figure 5. The  $J/\psi/DY$  ratio vs.  $E_T$ : averaged 1998 and 2000 data.

$E_{ZDC}$  (Fig. 7) show a suppression pattern similar to the one vs.  $E_T$  and, therefore, lead to the same conclusions. Inserts show the ratio “measured/expected”.

In order to compare the  $J/\psi$  suppression vs. centrality among different systems we introduce the average path  $L$  in nuclear matter, which is computed in each centrality class (or p+A system) with a Glauber approach. The Pb+Pb data on  $J/\psi/DY$  are shown together with the p+A data mentioned previously and the NA38 S+U data, rescaled to 158 GeV/nucleon, in Fig. 8 and, after division by the normal nuclear absorption curve, in Fig. 9. Figures 8 and 9 allow us a new conclusion, namely that  $J/\psi$  absorption in the S+U system is indeed compatible with normal nuclear absorption, as it is in peripheral Pb+Pb

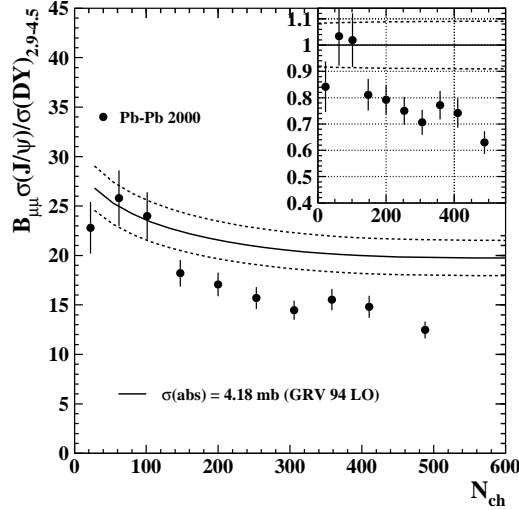


Figure 6. The  $J/\psi/DY$  ratio vs.  $N_{ch}$  from NA50 year 2000 data.

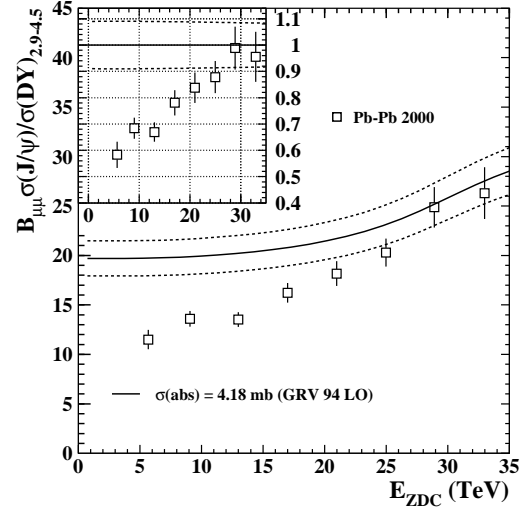


Figure 7. The  $J/\psi/DY$  ratio vs.  $E_{ZDC}$  for NA50 year 2000 data.

collisions. For S+U and Pb+Pb collisions we present in Fig. 10 the measured/expected ratio also as a function of energy density, evaluated in the Bjorken approach [9].

#### 4.2. Centrality dependence of the $\psi'/DY$ cross-section ratio

We have performed the same analysis on the  $\psi'/Drell\text{-}Yan$  cross-section ratio, which was extracted using the invariant mass spectrum fitting procedure described above. The combined 1998 and 2000 Pb+Pb data sample was divided in 7 centrality bins, in order to obtain a reasonable statistical error on the  $\psi'/DY$  ratio. A similar analysis has been performed on NA38 S+U data and on the three NA50 p+A data samples. The results are presented together in Fig. 11 as a function of the average path in nuclear matter,  $L$ .

We observe a quite different behaviour between the p+A systems and the other ones; by performing a Glauber fit to the p+A data only we extract a value of  $\sigma_{abs,pA}^{\psi'} = 7.6 \pm 1.1$  mb for the  $\psi'$  absorption in nuclear matter, larger than the one found for the  $J/\psi$ . The absorption curve deduced from p+A data is shown in Fig. 11 together with the error from the Glauber fit: we note that already in the S+U system the  $\psi'/DY$  ratio deviates from normal nuclear absorption. In fact, both Pb+Pb and S+U data show approximately the same absorption of  $\psi'$ , much larger than the one observed in p+A.

#### 4.3. Transverse momentum dependence of the $J/\psi$ suppression

In order to obtain further details on the  $J/\psi$  absorption pattern we have studied its  $p_T$  dependence. We have defined the  $p_T$ -dependent ratio  $F(E_T; p_{Ti}) = N_\psi(E_T; p_{Ti})/N_{DY}(E_T)$  in each of 11  $J/\psi$   $p_T$  bins and for 5 centrality bins defined by  $E_T$ . It must be noted that  $N_{DY}(E_T)$  refers to  $p_T$ -integrated Drell-Yan for a  $p_T$ -independent normalization just proportional to the number of nucleon-nucleon collisions in each  $E_T$  bin. The ratio  $F(E_T; p_{Ti})$  is shown as a function of centrality in Fig. 12 for the 3 lowest  $p_T$  bins (top left) and for the 3 highest  $p_T$  ones (bottom left). While the low  $p_T$  bins show the typical pattern of anomalous suppression, the high  $p_T$  ones are relatively flat vs. centrality, indicating that the anomalous suppression is indeed concentrated at low  $p_T$ .

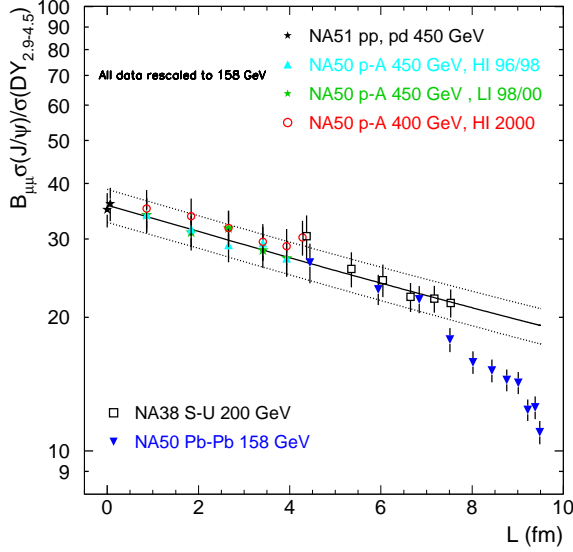


Figure 8. The  $J/\psi/DY$  ratio vs.  $L$  for p+A, S+U and Pb+Pb systems.

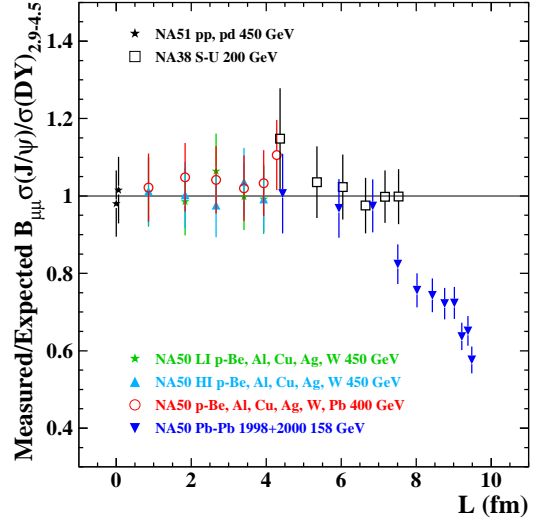


Figure 9. Measured/expected  $J/\psi/DY$  ratio vs.  $L$ .

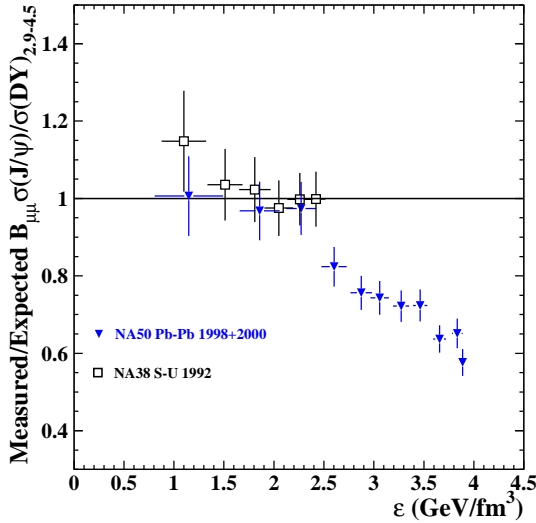


Figure 10. Measured/expected  $J/\psi/DY$  ratio vs. energy density.

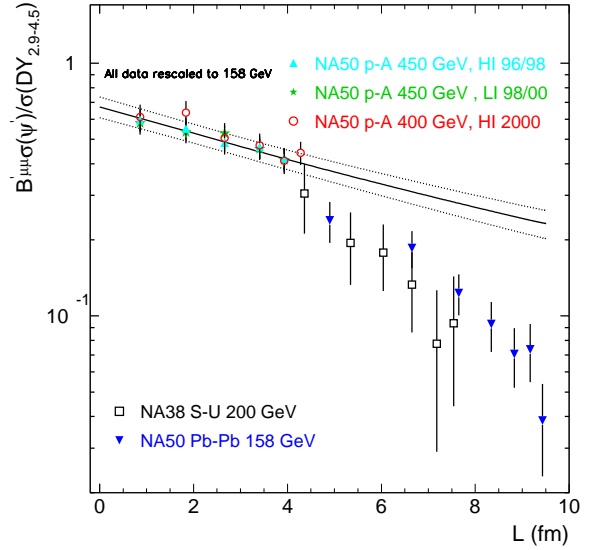


Figure 11. Measured/expected  $\psi'/DY$  ratio vs.  $L$ .

We have also defined the  $p_T$ -dependent “central-to-peripheral” ratios as  $R_{CP}^i(p_T) = (N_{\psi,i}(p_T)/N_{DY,i})/(N_{\psi,1}(p_T)/N_{DY,1})$ , where  $i = 2, 5$  denotes bins of increasing centrality and  $i = 1$  the most peripheral one. The four  $R_{CP}^i(p_T)$  ratios are shown vs.  $p_T$  in Fig. 12 (right): we observe again that the anomalous suppression of the  $J/\psi$  is concentrated at low  $p_T$ , while for  $p_T > 3.5$  GeV/ $c$  the centrality dependence (if any) is very weak.

Finally, we have fit the transverse mass distributions  $dN/dM_T$  of the  $J/\psi$  in each of 11 centrality bins (selected on the basis of  $E_T$ ) with a thermal model  $M_T^2 K_1(M_T/T)$ , extracting the effective temperature  $T$  from the fit. We note that  $T$  and  $\langle p_T^2 \rangle$  are linearly correlated, apart from small fluctuations due to the fitting procedure.

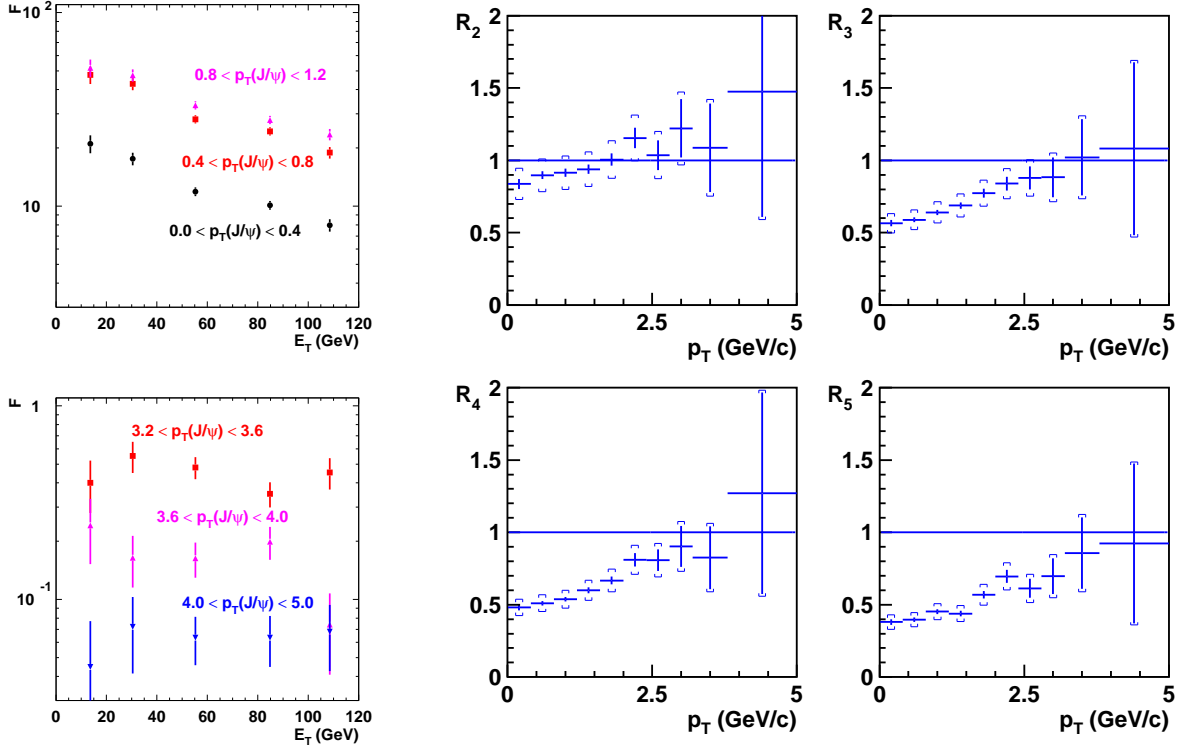


Figure 12. Left: the ratio  $F(E_T; p_{Ti})$  vs.  $E_T$  for the three lowest (top) and the three highest (bottom)  $p_T$  bins ( $p_T$  values in GeV/c). Right: the ratio  $R_{CP}^i(p_T)$  vs.  $p_T$  in centrality bins  $i = 2, 3, 4, 5$ .

Fig. 13 shows the behaviour of  $\langle p_T^2 \rangle$  as a function of  $L$  for p+A, S+U and Pb+Pb systems (at different energies). All systems show a linear increase with  $L$  of  $\langle p_T^2 \rangle$  and  $T$ , which is currently attributed to multiple scattering of initial partons, gluons in the case of the  $J/\psi$ .

A good phenomenological description is obtained with the expression  $\langle p_T^2 \rangle(L) = \langle p_T^2 \rangle_{pp} + a_{gN}L$ , with an energy-dependent proton-proton coefficient  $\langle p_T^2 \rangle_{pp}$  and a common slope:  $a_{gN} = 0.081 \pm 0.002 \text{ GeV}^2/c^2/\text{fm}$ .

A closer examination of the Pb+Pb results vs. centrality, expressed in this case by the  $E_T$  variable, is presented in Fig. 14. By using the expanded scale given by  $E_T$  we actually observe a saturation of  $\langle p_T^2 \rangle$  and of  $T$  for the  $J/\psi$  in central Pb+Pb collisions.

## 5. CONCLUSIONS

We have presented results on charmonium production and suppression at the CERN SPS energies based on high precision NA50 data. With a new determination of the normal nuclear absorption, derived from p+A collisions only (data taken at 200, 400 and 450 GeV), we have found the following features concerning  $J/\psi$  and  $\psi'$  at 158 GeV/nucleon. The anomalous suppression of  $J/\psi$  in semicentral and central Pb+Pb collisions has been confirmed (using the standard  $J/\psi$  / DY method) with higher accuracy than previously, by combining the 1998 and 2000 data (accuracy is ultimately limited by the available Drell-

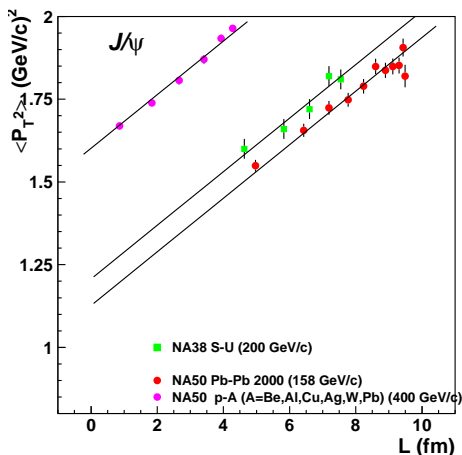


Figure 13. Average  $J/\psi$   $p_T^2$  vs.  $L$  for p+A, S+U and Pb+Pb collisions.

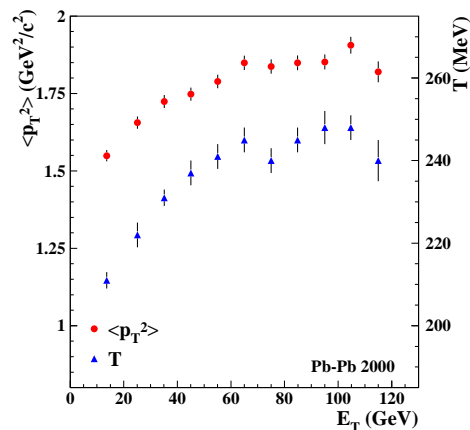


Figure 14. Average  $p_T^2$  and temperature vs.  $E_T$  for  $J/\psi$  in Pb+Pb collisions.

Yan statistics). We have determined that the anomalous suppression of the  $J/\psi$  mostly happens at low  $J/\psi$  transverse momentum; by fitting the  $J/\psi$   $p_T$  distributions in Pb+Pb we have observed an initial increase followed by a saturation for central collisions, for both  $\langle p_T^2 \rangle$  and temperature. We have found that in peripheral Pb+Pb collisions, but also in all of the S+U interactions (at 200 GeV/nucleon), the  $J/\psi$  production is in agreement with normal nuclear absorption. We have observed that the  $\psi' / DY$  ratio indicates the same suppression pattern in S+U and in Pb+Pb collisions, and one which is very different from normal  $\psi'$  absorption in p+A collisions.

## REFERENCES

1. T. Matsui and H. Satz, Phys. Lett. B178 (1986) 416.
2. L. Maiani, these proceedings; M. Nardi, these proceedings.
3. M.C. Abreu et al. (NA38 Collaboration), Phys. Lett. B449 (1999) 128 and B466 (1999) 408.
4. M.C. Abreu et al. (NA50 Collaboration), Phys. Lett. B410 (1997) 337.
5. M.C. Abreu et al. (NA50 Collaboration), Phys. Lett. B450 (1999) 456.
6. L. Ramello et al. (NA50 Collaboration), Nucl. Phys. A715 (2003) 243.
7. G. Borges et al. (NA50 Collaboration), J. Phys. G: Nucl. Part. Phys. 30 (2004) S1351.
8. H. Santos et al. (NA50 Collaboration), J. Phys. G: Nucl. Part. Phys. 30 (2004) S1175.
9. B. Alessandro et al. (NA50 Collaboration), Eur. Phys. J. C39 (2005) 335.
10. L. Kluberg, Eur. Phys. J C43 (2005) 145.
11. P. Cortese (NA50 Collaboration), these proceedings.
12. M.C. Abreu et al. (NA50 Collaboration), Phys. Lett. B410 (1997) 327.
13. M.C. Abreu et al. (NA50 Collaboration), Phys. Lett. B553 (2003) 167.
14. B. Alessandro et al. (NA50 Collaboration), Eur. Phys. J. C33 (2004) 31.
15. G. Borges et al. (NA50 Collaboration), Eur. Phys. J C43 (2005) 161.
16. M. Glück et al., Z. Phys. C67 (1995) 433.
17. J. Badier et al., Z. Phys. C20 (1983) 101.
18. A. Trzcinska et al., Phys. Rev. Lett. 87 (2001) 082501.